7730–7739 Nucleic Acids Research, 2011, Vol. 39, No. 17 Published online 17 June 2011
doi:10.1093/nar/gkr446

Identification of a signature motif for the eIF4a3–SECIS interaction

Michael E. Budiman[1], Jodi L. Bubenik[1] and Donna M. Driscoll[1,2,*]

[1]Department of Cell Biology, Lerner Research Institute, Cleveland Clinic, 9500 Euclid Ave., NC-10 and [2]Department of Molecular Medicine, Cleveland Clinic Lerner College of Medicine of Case Western Reserve University, Cleveland, OH 44195, USA

Received March 8, 2011; Revised May 12, 2011; Accepted May 13, 2011

ABSTRACT

eIF4a3, a DEAD-box protein family member, is a component of the exon junction complex which assembles on spliced mRNAs. The protein also acts as a transcript-selective translational repressor of selenoprotein synthesis during selenium deficiency. Selenocysteine (Sec) incorporation into selenoproteins requires a Sec Insertion Sequence (SECIS) element in the 3′ untranslated region. During selenium deficiency, eIF4a3 binds SECIS elements from non-essential selenoproteins, preventing Sec insertion. We identified a molecular signature for the eIF4a3-SECIS interaction using RNA gel shifts, surface plasmon resonance and enzymatic foot printing. Our results support a two-site interaction model, where eIF4a3 binds the internal and apical loops of the SECIS. Additionally, the stability of the complex requires uridine in the SECIS core. In terms of protein requirements, the two globular domains of eIF4a3, which are connected by a linker, are both critical for SECIS binding. Compared to full-length eIF4a3, the two domains *in trans* bind with a lower association rate but notably, the uridine is no longer important for complex stability. These results provide insight into how eIF4a3 discriminates among SECIS elements and represses translation.

INTRODUCTION

Eukaryotic initiation factor 4a3 (eIF4a3), a member of the DEAD-box protein family of RNA-dependent ATPases, is a nuclear/cytoplasmic shuttling protein (1). The canonical function of eIF4a3 is to bind spliced mRNAs 20–24-nt upstream of exon–exon junctions (2–5). As part of the exon junction complex (EJC), eIF4a3 serves as a critical link between pre-mRNA-splicing and post-splicing events that occur in the cytoplasm, including mRNA degradation, translation and localization (4,6). Biochemical and structural studies support a clamping model for the assembly of the exon junction core complex, which is organized around eIF4a3. The stable interaction of eIF4a3 with spliced mRNAs requires other EJC components, Magoh and Y14, which lock eIF4a3 in the RNA-bound conformation in an ATP-dependent manner (7–9).

In addition to its canonical function, eIF4a3 also acts as a transcript-specific repressor of selenoprotein mRNA translation during selenium deficiency (10). Selenoproteins are synthesized by a novel pathway, in which the UGA stop codon is recoded as selenocysteine (Sec). Incorporation of Sec into the growing polypeptide chain requires a Sec Insertion Sequence (SECIS) element in the 3′ untranslated region (UTR) of the transcript (11). The SECIS interacts with SECIS-binding protein 2 (SBP2), an essential factor for UGA recoding (12,13).

The expression of the mammalian selenoproteome is regulated by selenium status. When selenium becomes limiting, certain selenoproteins are synthesized at the expense of others (14,15). We established that eIF4a3 contributes to the hierarchy of selenoprotein expression. During selenium deficiency, there is an increase in eIF4a3 protein, which is required for the selective translational repression of a subset of selenoproteins (10). eIF4a3 binds to SECIS elements from Glutathione Peroxidase 1 (GPx1) and Methionine *R*-Sulfoxide Reductase (MsrB1; also known as SelR or SelX), but not from Phospholipid Hydroperoxide Glutathione Peroxidase (PHGPx) and Thioredoxin Reductase 1 (TrxR1) (10). GPx1 and MsrB1 are considered non-essential selenoproteins since their expression is reduced in selenium deficiency (16–19). Furthermore, disruption of the GPx1 and MsrB1 genes in mice results in a minimal phenotype (20–22). In contrast, PHGPx and TrxR1 are considered essential housekeeping selenoproteins. These selenoproteins are preserved in selenium deficiency (19,23–25) and the corresponding knockout mice have an embryonic

*To whom correspondence should be addressed. Tel: +1 216 445 9758; Fax: +1 216 444 9404; Email: driscod@ccf.org

lethal phenotype (26,27). Our published results support a model in which the interaction of eIF4a3 with the GPx1 and MsrB1 SECIS elements prevents binding of SBP2, thus inhibiting the synthesis of these two non-essential selenoproteins when selenium is limiting (10). Interestingly, the helicase activity of eIF4a3 was not required for this function, which suggests that unwinding of the SECIS element is not the mechanism of action (10).

How eIF4a3 and other DEAD-box proteins identify their cognate binding sites in RNA targets is not well understood. Unlike the non-specific interaction of eIF4a3 with spliced mRNAs, the selective SECIS-binding activity of eIF4a3 does not require other proteins. Eukaryotic SECIS elements adopt a hairpin structure which is composed of two helices separated by an internal loop (28). Previous studies utilizing chemical and enzymatic probing as well as mutagenesis have divided these elements into two distinct classes of structures (29,30). Type 1 elements contain a relatively large apical loop, while type 2 elements have a small loop, a mini helix and a bulge in their apical region. GPx1 and MsrB1, which interact with eIF4a3, are type 1 elements, whereas PHGPx and TrxR1, which do not bind eIF4a3, are type 2 elements (Figure 1A). Our published mutagenesis studies showed that the internal loop of the SECIS element was necessary, but not sufficient to mediate eIF4a3 binding, which suggests that the protein recognizes additional determinants (10). Thus, we proposed that eIF4a3 might preferentially bind to SECIS elements that contain a large apical loop.

In this study, we used biochemical and biophysical approaches to identify a molecular signature of the eIF4a3–SECIS interaction. Our results show that high affinity binding of eIF4a3 requires both the internal loop and the apical loop of the SECIS element. Unexpectedly, we found that a uridine base located at a particular position within the SECIS core is also critical for the stability of the complex. The requirement for two loops in the SECIS prompted us to investigate the structure of eIF4a3, which is composed of two domains and a flexible linker. Our results suggest that the N- and C-terminal domains (NTD and CTD, respectively) of eIF4a3 bind cooperatively to the SECIS and that the U in the SECIS core is only required when the two domains are linked *in cis*. We propose a two-site interaction model, which explains how eIF4a3 discriminates among SECIS elements and prevents SBP2 binding.

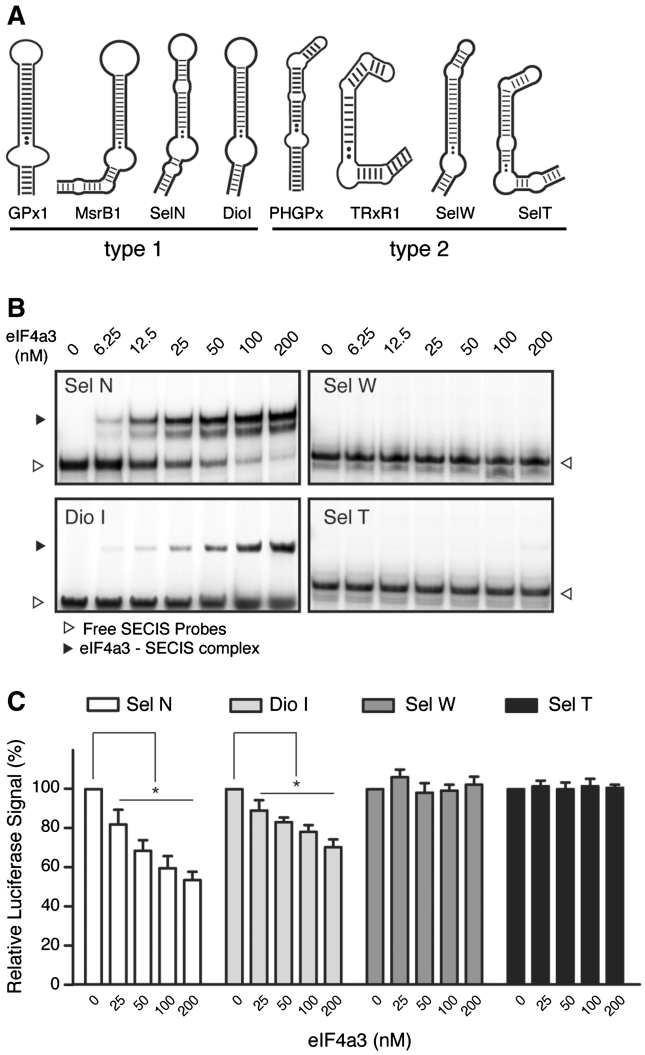

Figure 1. eIF4a3 binds to SECIS elements with a large apical loop. (**A**) Illustration of the structures of various type 1 and 2 SECIS elements. (**B**) REMSA analysis. The ^{32}P-labeled SelN, Dio1, SelW or SelT SECIS elements were incubated with increasing amounts of eIF4a3 as indicated. Samples were analyzed by native gel electrophoresis and autoradiography. (**C**) *In vitro* UGA-recoding assays. Luciferase reporter mRNAs containing a UGA codon in the open reading frame and the indicated SECIS element in the 3′-UTR were *in vitro* translated in the presence of varying amounts of eIF4a3. The luciferase results were expressed relative to reactions that were performed in the absence of eIF4a3. Statistically significant differences ($P < 0.005$) are denoted by an asterisk.

MATERIALS AND METHODS

Reagents

Constructs containing the various wild-type SECIS elements were previously described (10,31). Mutations in the GPx1 SECIS were introduced using QuikChange II Site Directed Mutagenesis Kit (Stratagene). Non-labeled, internally ^{32}P-labeled and biotinylated SECIS RNAs were transcribed from linear plasmid DNA using T7-Ampliscribe, RiboScribe RNA Probe and Flash Biotin-RNA transcription kits (Epicentre), respectively. The 5′-end-labeled SECIS RNAs were produced as described (32). The luciferase reporter construct containing the GPx1 SECIS was previously generated (10). Additional constructs were generated by replacing the GPx1 SECIS in the 3′-UTR with other SECIS elements. Recombinant rat eIF4a3 was cloned, expressed and purified as described (10). Nucleotides encompass amino acids 1–245 (NTD) or amino acids 246–411 (CTD) of the rat eIF4a3 were generated by PCR amplification of bases 61–795 or 796–1293 of the rat eIF4a3 mRNA, respectively (accession no NM_001100158.2). The PCR products were cloned into pET101 TOPO vector (Invitrogen).

The recombinant NTD and CTD were expressed and purified similar to the recombinant full-length eIF4a3.

RNA-binding assays

REMSA experiments were done as previously described (10). Surface plasmon resonance (SPR) analyses were carried out using a BIACORE 3000 biosensor system. Briefly, 200 response units of biotinylated SECIS RNAs were immobilized on a sensor chip SA (GE Healthcare). To determine the association rate, varying concentrations of eIF4a3 were automatically injected at flow rate of 25 µl/min for 180 sec. Following the association step, the formed complex was monitored for 210 sec to determine its dissociation rate. A flow cell without immobilized RNA was subjected to same treatment and used as a control. The signal generated in the control flow cell was subtracted from the experimental signal to correct for refractive index changes and non-specific binding. The sensorgrams were fit to a simultaneous K_A/K_D model to derive kinetic parameters using Biaevaluation software ver. 4.0.1 (GE Healthcare). Each experiment was performed in duplicate with similar results, and representative sensorgrams are shown in the figures.

UGA recoding assay

In vitro UGA-recoding assays were performed as described (10). Luciferase activities were measured using Victor3 Multilabel Plate Reader (Perkin Elmer). Results were calculated from three independent experiments which were analyzed in triplicate and are represented as mean ± SD. Statistical analyses were performed using Prism 5 (Graphpad).

Enzymatic RNA footprinting

The 5′-end-labeled SECIS RNAs were incubated without or with recombinant eIF4a3 in 20 µl REMSA buffer (10) containing 1 µl of 0.1 µg/ml RNase A or 0.01 U/µl RNase V1 (Ambion). After 10 min at 4°C, the reactions were terminated using 20 µl of inactivation buffer (Ambion), phenol chloroform extracted and ethanol precipitated. The products were separated in 8% acrylamide/8 M urea gels, which were dried and subjected to autoradiography. Nucleotide positions were identified by alignment with the sequencing ladders, which were obtained by denaturing the 5′-end-labeled SECIS RNAs in RNA sequencing buffer (Ambion) containing 7 M urea. The samples were incubated with 1 µl 0.1 U of RNase T1 (G bases) or 1 µl of 0.1 µg/ml RNase A (C and U bases). Footprinting experiments were performed twice for each SECIS element with similar results.

RESULTS

eIF4a3 binds to SECIS elements that contain a large apical loop

Based on our previous studies, we hypothesize that eIF4a3 binds preferentially to type 1 SECIS elements which contain a large apical loop. To investigate this possibility, we selected two type 1 SECIS elements, Selenoprotein N (SelN) and Deiodinase 1 (Dio1), and two type 2 SECIS elements, Selenoprotein W (SelW) and Selenoprotein T (SelT) (Figure 1A). eIF4a3–SECIS interactions were analyzed using RNA electrophoretic mobility shift assays (REMSA). The ^{32}P-labeled SECIS RNAs were incubated with increasing amounts of eIF4a3 and the resulting RNA–protein complexes were analyzed by native gel electrophoresis. As shown in Figure 1B, eIF4a3 bound to the SelN and Dio1 SECIS RNAs in a dose-dependent manner. In contrast, we observed little or no interaction of eIF4a3 with the SelW and SelT SECIS RNAs, even at the highest protein concentration tested.

We previously used a luciferase reporter assay to show that eIF4a3 selectively inhibits the UGA-recoding activities of the GPx1 and MsrB1 SECIS elements in an *in vitro* translation system (10). This assay relies on a modified luciferase mRNA, which contains a UGA codon in the coding region and a SECIS element fused to its 3′-UTR. Synthetic RNAs are translated in rabbit reticulocyte lysate in the presence or absence of eIF4a3, and the translation products are analyzed for luciferase activity. This assay has been validated to be specific for Sec incorporation (33) and eIF4a3-mediated translational repression (10). As shown in Figure 1C, the addition of eIF4a3 reduced the luciferase signal from the reporter mRNA harboring either the SelN or Dio1 SECIS element in a dose-dependent manner. When eIF4a3 was added to 200 nM, we observed a ∼50% decrease in UGA recoding activity for the SelN SECIS and a ∼30% reduction for the Dio1 SECIS. The greater effect on SelN is consistent with the fact that eIF4a3 has a higher binding affinity for this SECIS element. The levels of inhibition observed here are similar to what we previously reported for GPx1 and MsrB1 (10). In agreement with the REMSA results, eIF4a3 did not inhibit the UGA-recoding activities of the SelW and SelT SECIS elements. These observations indicate that the SECIS-binding activity of eIF4a3 correlates with its ability to reduce UGA recoding.

Binding of eIF4a3 requires the internal and apical loops of the SECIS

Our current and previous observations suggested that binding of eIF4a3 may require both the internal and apical loops of the SECIS element. To gain insight into the dynamics of eIF4a3–SECIS complex formation, we analyzed the interaction of eIF4a3 with wild-type and mutant GPx1 SECIS RNAs by SPR. To assess the role of the internal loop, we tested mutant A (Figure 2A), in which the internal loop of the GPx1 SECIS is replaced with five Watson–Crick base pairs. We previously showed that this mutant did not bind eIF4a3 in a REMSA assay (10). To investigate the contribution of the apical loop to eIF4a3–SECIS complex formation, we replaced the 9-base loop in GPx1 SECIS with a 5-base loop (Figure 2A, mutant B).

Our SPR analyses showed that eIF4a3 interacts with the wild-type GPx1 SECIS with a K_D of 5.1 nM (Figure 2B), which is in agreement with our previous REMSA data (10). In contrast, the affinity of eIF4a3 for the PHGPx SECIS was only 5.13 µM (data not shown). As expected,

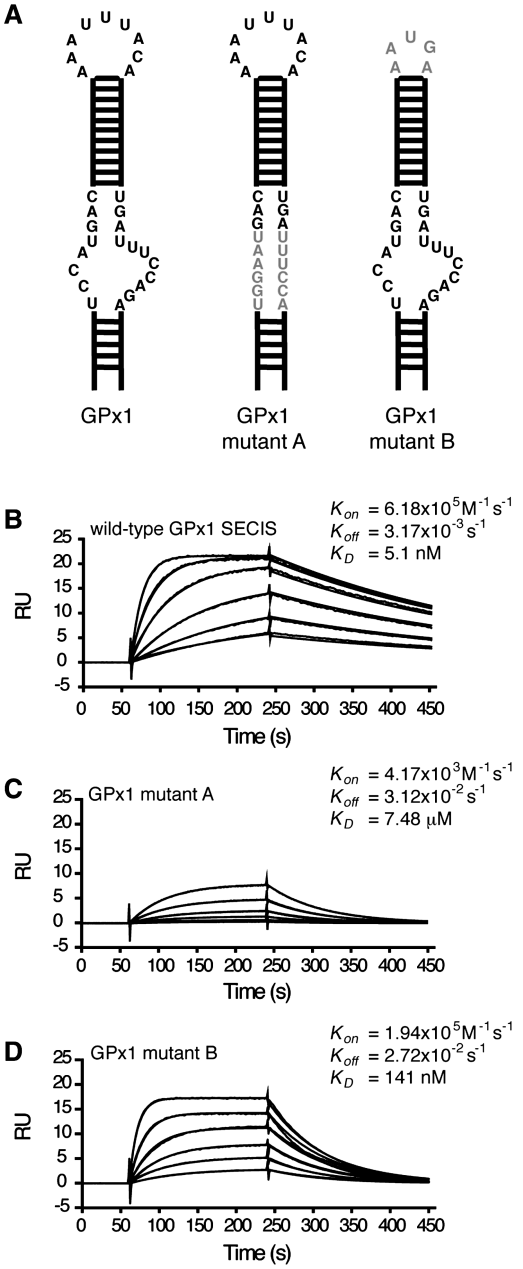

Figure 2. eIF4a3 binding requires both loops of the SECIS element. (**A**) Schematic representation of the wild-type GPx1 SECIS, the internal loop mutant (mutant A) and the apical loop mutant (mutant B). eIF4a3–SECIS interactions were analyzed by SPR and representative sensorgrams for the wild-type GPx1 SECIS (**B**), mutant A (**C**) or mutant B (**D**) RNAs are shown. Varying concentrations of eIF4a3 (ranging from 3.125 to 100 nM for the wild-type GPx1, from 100 nM to 3.2 μM for mutant A and from 25 to 800 nM for mutant B) were injected. Kinetic parameters were derived as described in 'Material and Methods' section.

closing the internal loop in mutant A reduced the affinity of eIF4a3 for the SECIS element by >1000-fold (Figure 2C). This defect in binding is mainly due to a 150-fold decrease in the association rate compared to the wild-type GPx1 SECIS. The apical loop is also an important determinant for binding since the affinity of eIF4a3 for mutant B was reduced by 30-fold (Figure 2D). Interestingly, this lower affinity is primarily caused by an increase in the dissociation rate compared to the wild-type GPx1 SECIS (2.72×10^{-2}/s versus 3.17×10^{-3}/s). Thus, while the internal loop is required to initiate eIF4a3–SECIS complex formation, the apical loop is needed to maintain the stability of the eIF4a3–SECIS interaction.

eIF4a3 protects both loops in the SECIS from enzymatic cleavage

In order to directly map the eIF4a3-binding site, we performed enzymatic RNA footprinting on various eIF4a3–SECIS complexes. Nucleotides involved in the eIF4a3–SECIS interaction were determined through partial digestion of the SECIS RNA, which was performed in the absence or presence of eIF4a3. We used RNase A, which cleaves at single-stranded C and U bases, or RNase V1, which cleaves at double-stranded regions. The cleavage patterns for the GPx1, MsrB1 and SelN SECIS elements are shown in Figure 3A–C, respectively. The results for all three SECIS elements are shown schematically in Figure 3D.

RNase A cleaved the native GPx1 SECIS in both the internal and apical loops, while RNase V1 resulted in cleavage at multiple positions in helices 1 and 2 (Figure 3A). These cleavage patterns are consistent with the previously published structure of the GPx1 SECIS (32). We also observed that the upper part of helix 2 (bases 28, 32 and 42–46) was not sensitive to RNase V1, possibly due to breathing in this region. Binding of eIF4a3 protected the GPx1 SECIS from enzymatic cleavage in two localized areas, which are centered on the internal loop and apical loop. The eIF4a3–SECIS complex was protected from RNase A cleavage in both the internal loop (bases 14, 15 and 58) and apical loop (bases 36–38, 40 and 42). In the presence of eIF4a3, RNase V1 no longer cleaves the regions flanking the internal loop, corresponding to helix 1 (bases 9–13, 64 and 65) and the SECIS core (bases 17, 18 and 55–57). Interestingly, the upper part of helix 2 (bases 28, 32 and 43–47) became sensitive to RNase V1 cleavage, which suggests that eIF4a3 may stabilize the base pairing in this region.

Analysis of the MsrB1 SECIS (Figure 3B) revealed that RNase A cleaved at multiple sites in the large apical loop as well as in the internal loop region, whereas RNase V1 cleaved the RNA in helices 1 and 2. We also noticed that part of the apical loop (bases 45–49) was sensitive to both RNase A and V1, suggesting that this region fluctuates between single- and double-stranded forms. This result is in agreement with the previous report that the MsrB1 SECIS equilibrates between the types 1 and 2 structures (29). Addition of eIF4a3 prevented RNase A from cleaving the MsrB1 SECIS at bases 13, 15 and 64 in the internal loop and bases 36–38 and 43, 45, 46 and 49 in the apical loop. In addition, RNase V1 digestion at bases 10–12, and 68–71 in helix 1 and at bases 17, 18 and 59 in the SECIS core were diminished upon eIF4a3 binding.

RNase digestion of the SelN SECIS element (Figure 3C) also resulted in cleavage patterns that were consistent with it being a type 1 element as shown in a previous study (29).

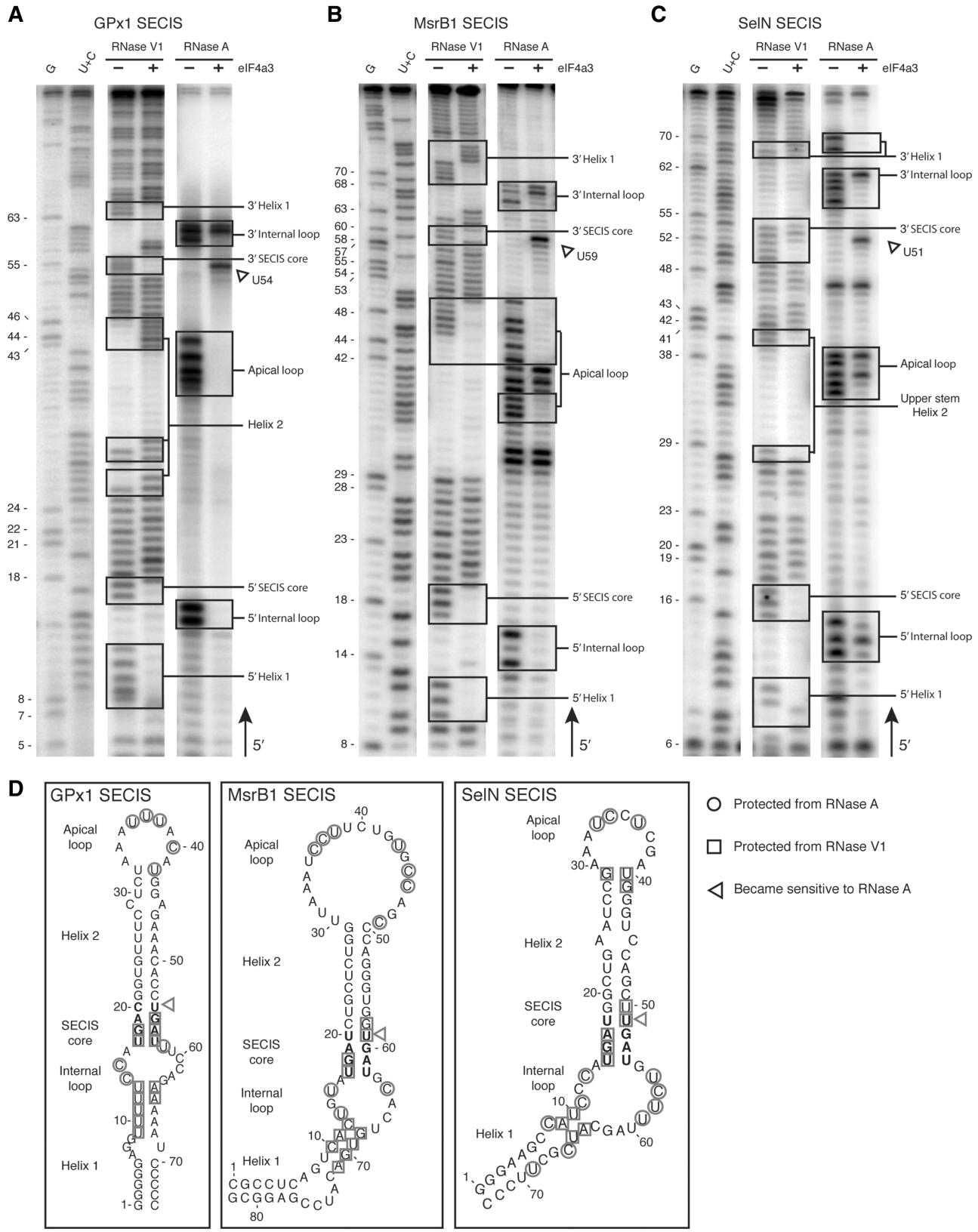

Figure 3. Enzymatic footprinting of eIF4a3–SECIS complexes. (**A**) The 5′-end-labeled GPx1 SECIS RNA, alone or in complex with eIF4a3, was partially cleaved with RNase A or V1. The products were analyzed by denaturing gel electrophoresis. The U+C and G ladders are shown. Guanine positions indicated on the left correspond to the numbering in Figure 3D. Boxes indicate changes in nucleotide sensitivity in the presence of eIF4a3. Identical experiments were performed with the MsrB1 (**B**) and SelN SECIS RNAs (**C**). Bands resulted from the RNAse A and V1 cleavage in the footprinting lanes migrate slightly slower compared to the sequencing lanes (**D**). Summary of the RNase cleavage sites affected by eIF4a3. Protections are indicated by open circle for the RNase A and open square for the RNase V1. Nucleotides that became sensitive to RNase A cleavage in the presence of eIF4a3 are indicated by open triangle.

In the presence of eIF4a3, the SelN SECIS was protected from RNase A cleavage in the apical loop (bases 33, 34 and 36) as well as in and around the internal loop (bases 8, 11, 13, 56–59, 63, 66 and 69). Additionally, bases 9, 10, 64 and 65 in helix 1 and bases 15–17, 50 and 51 in the SECIS core were protected from RNase V1 upon eIF4a3 addition.

Taken together, these results show that eIF4a3 interacts with the GPx1, MsrB1 and SelN SECIS elements in two distinct regions, which encompass the internal and the apical loops.

Stable binding of eIF4a3 requires a uridine in the SECIS core

Eukaryotic SECIS elements contain a quartet of non Watson–Crick base pairs, which form the SECIS core. The two sheared tandem G•A pairs (G•A/A•G) in the center of the core are highly conserved (Figure 3D) (12,34) and essential for SBP2 binding and UGA recoding. The other base pairs in the quartet vary between SECIS elements. Interestingly, the GPx1, SelN, MsrB1 and Dio1 SECIS elements all contain a 3′-U in the upper base pair of the SECIS core (Figure 3D, arrowhead). We noticed that this uridine (GPx1:U54, MsrB1:U59 and SelN:U51) became sensitive to RNase A upon eIF4a3 binding (Figure 3A–C, arrowhead). Inspection of the four SECIS elements that do not bind eIF4a3 showed that either a C or A base occupies this position. To test the hypothesis that this particular U might play a role in the eIF4a3–SECIS interaction, we mutated U54 in the GPx1 SECIS to C. This mutation was chosen since it did not inhibit Sec incorporation in transfected cells (35). Based on SPR analysis, the affinity of eIF4a3 for the U54 → C mutant was reduced by 90-fold (K_D of 435 nM) (Figure 4A) compared to the wild-type GPx1 SECIS (K_D of 5.1 nM, Figure 2A). Evaluation of its kinetic parameters showed that the association rate for the mutant (1.82×10^5/Ms) is only 4-fold lower compared to wild-type SECIS (6.18×10^5/Ms). Intriguingly, the dissociation rate from the U54 → C mutant RNA (1.58×10^{-2}/s) is 25-fold higher than the wild-type SECIS (3.17×10^{-2}/s). Thus, U54 is required to maintain a stable eIF4a3–SECIS interaction.

The U54 → C mutant was also analyzed in the luciferase reporter assay described above. In the absence of eIF4a3, the wild-type and mutant GPx1 SECIS elements recoded the UGA codon with similar efficiencies (Figure 4B). The difference in the levels of luciferase activity for the wild-type and mutant RNAs was not statistically significant. However, we found that the addition of exogenous eIF4a3 to the translation assay did not inhibit the UGA-recoding activity of the U54 → C mutant SECIS, even at the highest protein concentration tested (Figure 4B). These results suggest that a stable eIF4a3–SECIS complex is necessary to inhibit UGA recoding.

The two domains of eIFa3 bind the SECIS *in cis* and *in trans*

The structure of eIF4a3 resembles a dumbbell shape, with two compact domains connected by a flexible linker (7,8).

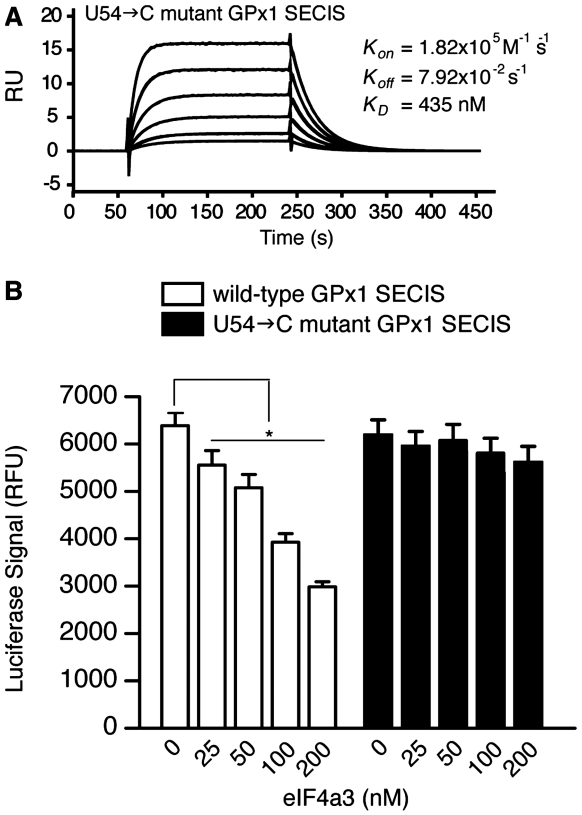

Figure 4. Uridine base in the SECIS core is required for stable eIF4a3 binding. (**A**) A representative sensorgram for the eIF4a3–U54 → C mutant GPx1 SECIS interaction is shown. Various concentrations of eIF4a3 (from 25 to 800 nM) were passed over a sensor chip immobilized with U54 → C mutant GPx1 SECIS. (**B**) Recoding assays were performed as described in Figure 1C using reporter constructs containing the wild-type GPx1 SECIS and the U54 → C mutant. Statistically significant differences ($P < 0.005$) are represented by an asterisk.

We wondered whether both domains are required for binding to the SECIS element. To test this hypothesis, we generated recombinant proteins that encompass either the NTD (amino acids 1–245) or CTD (amino acids 246–411) of rat eIF4a3. The recombinant proteins were analyzed by SPR either individually or together *in trans*. We found that the NTD bound to the GPx1 SECIS with a very low affinity (K_D of ~1 μM), while the interaction of the CTD with GPx1 SECIS was barely detectable (data not shown). Interestingly, when the two domains were analyzed *in trans*, the proteins bound the GPx1 SECIS with a K_D of 186 nM (Figure 5A). While the NTD and CTD added *in trans* exhibited a lower association rate (4.02×10^4/Ms, Figure 5A) compared to the full-length eIF4a3 (6.18×10^5/Ms, Figure 1B), this rate was notably higher compared to the NTD alone (1.03×10^3/Ms). Therefore, both domains of eIF4a3 are required for binding to the SECIS. However, the association rate is higher if the NTD and CTD are linked *in cis*.

We also analyzed the ability of the U54 → C mutant SECIS to interact with the NTD and CTD *in trans* (Figure 5B). Surprisingly, the affinity of the two domains for the mutant RNA (K_D of 202 nM) was

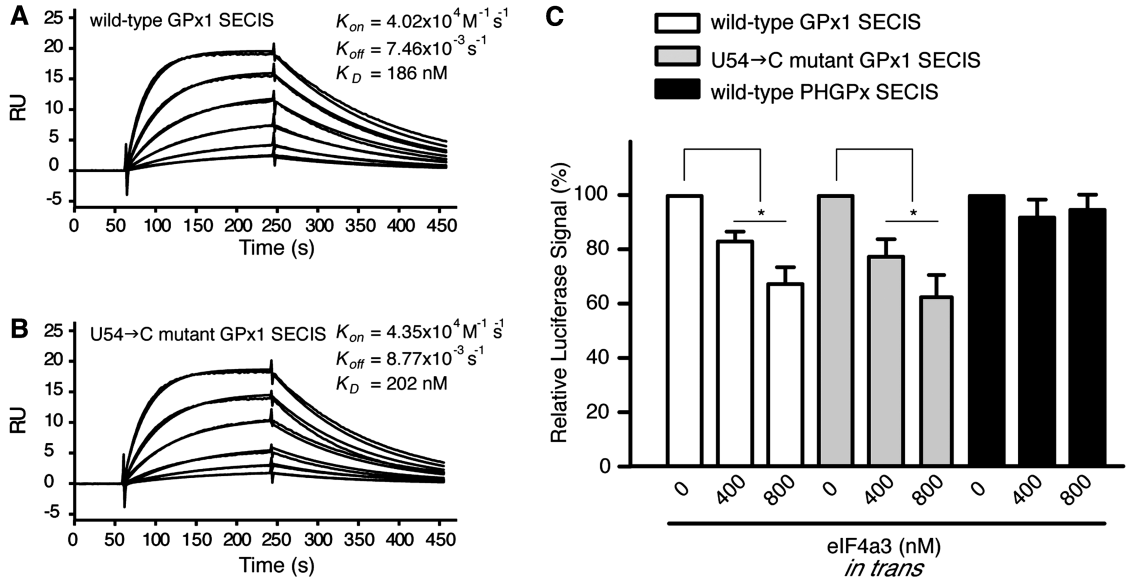

Figure 5. The two domains of eIF4a3 bind the GPx1 SECIS *in trans*. SPR analysis between the two domains of eIF4a3 *in trans* with the wild-type (**A**) and the U54 → C mutant (**B**) GPx1 SECIS are shown. eIF4a3 (from 25 to 800 nM) was injected to immobilized SECIS RNAs to determine the binding parameters. (**C**) *In vitro* recoding assays using reporter mRNAs containing a UGA codon in the open reading frame and a wild-type or U54 → C mutant GPx1 SECIS element in the 3′-UTR. The two domains of eIF4a3 were added to the assay *in trans* as indicated. Reporter mRNA harboring the wild-type PHGPx SECIS element was used as a control for selective inhibition. The luciferase results were expressed relative to reactions that were performed in the absence of eIF4a3. Statistically significant differences ($P < 0.005$) are denoted by an asterisk.

comparable to the affinity for the wild-type GPx1 SECIS (K_D of 186 nM). Furthermore, the U54 → C mutation had little effect on the dissociation rate of the NTD and CTD *in trans*. These results are in contrast to what we observed for the full-length protein. Thus, the requirement of U54 for the stability of the eIF4a3–SECIS complex only holds true when the NTD and CTD are tethered together by the linker.

In order to determine whether binding of the NTD and CTD *in trans* has functional consequences, we utilized the luciferase reporter assay. The two domains *in trans* inhibited the UGA-recoding activity directed by the wild-type GPx1 SECIS, but not by the PHGPx SECIS (Figure 5C). These observations suggest that the NTD and CTD *in trans* retained the selectivity of the *in cis* counterpart. Moreover, unlike the full-length eIF4a3, the NTD and CTD *in trans* were able to repress the UGA-recoding activity of the U54 → C mutant SECIS (Figure 5C).

DISCUSSION

We previously established that eIF4a3 is a selective translational repressor of two selenoproteins, GPx1 and MsrB1 (10). In this study, we identified two additional targets of eIF4a3 and characterized the motifs in the SECIS element that comprise a molecular signature for the eIF4a3–SECIS interaction. Our results provide an important insight into the mechanism by which eIF4a3 differentially recognizes a subset of selenoprotein mRNAs to inhibit their translation.

Our new observation is that eIF4a3 binds to the Dio1 and SelN SECIS elements is intriguing, as these two selenoproteins may perform non-essential functions, like GPx1 and MsrB1. The Dio1 knockout mouse has a mild phenotype (36) and human subjects with loss of function mutations in the SelN gene survive, albeit they developed a severe dystrophy or a congenital myopathy (37,38). In contrast, eIF4a3 did not bind to the SelW and SelT SECIS elements, which belong to a new selenoprotein family whose members may have a redox function (39). Although knockout mice for SelW and SelT are not available, these mRNAs may not be subject to translational regulation by eIF4a3 since they are reduced in selenium deficient livers (40). Taken together, our results suggest that eIF4a3 regulates a cohort of selenoproteins that belong to the non-essential category.

Using multiple biochemical and biophysical approaches, we identified three motifs in the SECIS that are necessary for eIF4a3–SECIS complex formation: the internal loop, the apical loop and the uridine located in the 3′-upper base pair of the SECIS core. This molecular signature may explain how eIF4a3 preferentially interacts with type 1 SECIS elements. Kinetic studies revealed that each motif plays a specific role in facilitating eIF4a3 binding. While the internal loop is required for recognition, the apical loop and the uridine in the SECIS core are crucial for maintaining complex stability. The specificity of eIF4a3–SECIS interaction is largely generalizable across species. Database and structural analyses of the SECIS elements from the eight selenoproteins investigated for eIF4a3 binding suggest that there is structural conservation of each element in rat, mouse and human (Supplementary Table S1). SECIS elements from PHGPx, TrxR1, SelW and SelT, which do not interact

with eIF4a3, adopt the type 2 structure with no nucleotide conservation at the 3′-upper base pair of the SECIS core in rat, mouse and human. On the other hand, SECIS elements from GPx1, MsrB1, SelN and Dio1, adopt the type 1 structure with a conserved uridine at the 3′-upper base pair of the SECIS core. One exception is the SECIS element from human MsrB1, which is predicted to be a type 2 structure based on SECISearch (41), but has been shown to equilibrate between the types 1 and 2 structures based on the enzymatic and chemical probing experiments (29). In addition, the 3′-upper base pair of the human MsrB1 SECIS contains a guanine instead of uridine. While the possibility that eIF4a3 may interact with type 1 element containing a guanine has not been investigated, we believe that the less conserved MsrB1 SECIS element is more likely to represent its complex regulation. Previously, we have shown that mouse MsrB1 SECIS element interacts with both eIF4a3 (10), a negative regulator, as well as nucleolin (31), a positive regulator of selenoprotein mRNA translation. Furthermore, there may be differences in the regulation of MsrB1 between human and rodents.

Our studies also provide additional insight into the mechanism by which eIF4a3 prevents Sec incorporation. We previously showed that SBP2 could not bind to an eIF4a3-bound SECIS element (10). Based on a mutation in which the internal loop of the GPx1 SECIS was closed, we previously suggested that eIF4a3 might interfere with binding of SBP2 by physically preventing this interaction (10). The results presented here support this model of steric hindrance. Our RNA-footprinting analyses demonstrate that eIF4a3 protects nucleotides in the internal loop and SECIS core. These regions overlap with the previously characterized binding site of SBP2 (32).

Given that the internal and apical loops of the SECIS are required for the eIF4a3–SECIS interaction, we propose a two-site binding model. Structurally, eIF4a3 adopts a dumbbell shape consisting of two domains connected by a linker, similar to other DEAD-box protein family members, including eIF4a1. Previous SELEX experiments against eIF4a1 identified a high affinity RNA aptamer containing two loops, which are both required for efficient recognition by eIF4a1 (42). The aptamer may lock the two domains of eIF4A1 together through an 'induced fit' mechanism, thus triggering a conformational change in favor of the RNA-bound form. It is intriguing to speculate that the type 1 SECIS elements analyzed in our study represent a natural example of an RNA aptamer that immobilizes a DEAD-box protein. In this model, one domain of eIF4a3 may interact with the internal loop while the other domain of the protein binds to the apical loop of the SECIS. Our data showed that the *in trans* NTD and CTD of eIF4a3 bind to the SECIS with higher affinity compared to the NTD alone. These observations imply that the presence of the CTD facilitates complex formation, which suggest that the NTD and CTD of eIF4a3 bind the SECIS element in a cooperative manner.

Our finding that the uridine in the SECIS core is important for eIF4a3 binding when the NTD and CTD are present *in cis* but not *in trans* was somewhat surprising. Thus, we envision that the binding of eIF4a3 to the two distant sites in the SECIS may induce a bend or conformational change in the RNA. Such bending of the RNA has been previously observed in the crystal structures of the eIF4a3–RNA complex and other DEAD-box protein–RNA complexes (7–9,43,44). The change in nuclease sensitivity of the uridine in the SECIS core may be a consequence of accommodating such a structural alteration, presumably by relieving a torsional constraint.

Finally, our studies may have broader implications for other functions of eIF4a3. Although it has been believed that EJC formation is a constitutive consequence of splicing, a recent study from the LeHir group suggested that an EJC-like structure assembles on some but not all splice junctions (45). This association depends on an unidentified *cis*-acting element in the pre-mRNA. Considering that eIF4a3 is directly in contact with the RNA in the EJC core, the eIF4a3–SECIS signature that we have identified in this study may aid future investigation into the mechanism of sequence-dependent EJC deposition.

SUPPLEMENTARY DATA

Supplementary Data are available at NAR Online.

ACKNOWLEDGEMENTS

M.E.B. designed and performed experiments, analyzed data, and wrote the manuscript; J.L.B. analyzed data, gave conceptual advice, and edited the manuscript; and D.M.D. designed experiments; analyzed data, and wrote the manuscript. We thank Abby Bifano, Anne Cheever and Angela Miniard for helpful discussions and critical reading of the article.

FUNDING

National Institutes of Health (grants RO1DK078591 to D.M.D. and F32DK083154 to M.E.B.); Shared Instrumentation (grant RR016789-01A1 to S.P.Y. in the Molecular Biotechnology Core is for the Biacore 3000 experiments). Funding for open access charge: National Institutes of Health (grants RO1DK078591).

Conflict of interest statement. None declared.

REFERENCES

1. Li,Q., Imataka,H., Morino,S., Rogers,G.W. Jr, Richter-Cook,N.J., Merrick,W.C. and Sonenberg,N. (1999) Eukaryotic translation initiation factor 4AIII (eIF4AIII) is functionally distinct from eIF4AI and eIF4AII. *Mol. Cell. Biol.*, **19**, 7336–7346.
2. Chan,C.C., Dostie,J., Diem,M.D., Feng,W., Mann,M., Rappsilber,J. and Dreyfuss,G. (2004) eIF4A3 is a novel component of the exon junction complex. *RNA*, **10**, 200–209.
3. Shibuya,T., Tange,T.O., Sonenberg,N. and Moore,M.J. (2004) eIF4AIII binds spliced mRNA in the exon junction complex and is essential for nonsense-mediated decay. *Nat. Struct. Mol. Biol.*, **11**, 346–351.
4. Palacios,I.M., Gatfield,D., St Johnston,D. and Izaurralde,E. (2004) An eIF4AIII-containing complex required for mRNA

localization and nonsense-mediated mRNA decay. *Nature*, **427**, 753–757.
5. Ferraiuolo,M.A., Lee,C.S., Ler,L.W., Hsu,J.L., Costa-Mattioli,M., Luo,M.J., Reed,R. and Sonenberg,N. (2004) A nuclear translation-like factor eIF4AIII is recruited to the mRNA during splicing and functions in nonsense-mediated decay. *Proc. Natl Acad. Sci. USA*, **101**, 4118–4123.
6. Tange,T.O., Nott,A. and Moore,M.J. (2004) The ever-increasing complexities of the exon junction complex. *Curr. Opin. Cell Biol.*, **16**, 279–284.
7. Bono,F., Ebert,J., Lorentzen,E. and Conti,E. (2006) The crystal structure of the exon junction complex reveals how it maintains a stable grip on mRNA. *Cell*, **126**, 713–725.
8. Andersen,C.B., Ballut,L., Johansen,J.S., Chamieh,H., Nielsen,K.H., Oliveira,C.L., Pedersen,J.S., Seraphin,B., Le Hir,H. and Andersen,G.R. (2006) Structure of the exon junction core complex with a trapped DEAD-box ATPase bound to RNA. *Science*, **313**, 1968–1972.
9. Ballut,L., Marchadier,B., Baguet,A., Tomasetto,C., Seraphin,B. and Le Hir,H. (2005) The exon junction core complex is locked onto RNA by inhibition of eIF4AIII ATPase activity. *Nat. Struct. Mol. Biol.*, **12**, 861–869.
10. Budiman,M.E., Bubenik,J.L., Miniard,A.C., Middleton,L.M., Gerber,C.A., Cash,A. and Driscoll,D.M. (2009) Eukaryotic initiation factor 4a3 is a selenium-regulated RNA-binding protein that selectively inhibits selenocysteine incorporation. *Mol. Cell*, **35**, 479–489.
11. Berry,M.J., Banu,L., Chen,Y.Y., Mandel,S.J., Kieffer,J.D., Harney,J.W. and Larsen,P.R. (1991) Recognition of UGA as a selenocysteine codon in type I deiodinase requires sequences in the 3′ untranslated region. *Nature*, **353**, 273–276.
12. Copeland,P.R., Fletcher,J.E., Carlson,B.A., Hatfield,D.L. and Driscoll,D.M. (2000) A novel RNA binding protein, SBP2, is required for the translation of mammalian selenoprotein mRNAs. *EMBO J.*, **19**, 306–314.
13. Squires,J.E., Stoytchev,I., Forry,E.P. and Berry,M.J. (2007) SBP2 binding affinity is a major determinant in differential selenoprotein mRNA translation and sensitivity to nonsense-mediated decay. *Mol. Cell. Biol.*, **27**, 7848–7855.
14. Behne,D., Hilmert,H., Scheid,S., Gessner,H. and Elger,W. (1988) Evidence for specific selenium target tissues and new biologically important selenoproteins. *Biochim. Biophys. Acta.*, **966**, 12–21.
15. Hill,K.E., Lyons,P.R. and Burk,R.F. (1992) Differential regulation of rat liver selenoprotein mRNAs in selenium deficiency. *Biochem. Biophys. Res. Commun.*, **185**, 260–263.
16. Bermano,G., Nicol,F., Dyer,J.A., Sunde,R.A., Beckett,G.J., Arthur,J.R. and Hesketh,J.E. (1996) Selenoprotein gene expression during selenium-repletion of selenium-deficient rats. *Biol. Trace Elem. Res.*, **51**, 211–223.
17. Moskovitz,J. and Stadtman,E.R. (2003) Selenium-deficient diet enhances protein oxidation and affects methionine sulfoxide reductase (MsrB) protein level in certain mouse tissues. *Proc. Natl Acad. Sci. USA*, **100**, 7486–7490.
18. Novoselov,S.V., Kim,H.Y., Hua,D., Lee,B.C., Astle,C.M., Harrison,D.E., Friguet,B., Moustafa,M.E., Carlson,B.A., Hatfield,D.L. *et al.* (2010) Regulation of selenoproteins and methionine sulfoxide reductases A and B1 by age, calorie restriction, and dietary selenium in mice. *Antioxid. Redox. Signal*, **12**, 829–838.
19. Weiss Sachdev,S. and Sunde,R.A. (2001) Selenium regulation of transcript abundance and translational efficiency of glutathione peroxidase-1 and -4 in rat liver. *Biochem. J.*, **357**, 851–858.
20. Cheng,W.H., Ho,Y.S., Ross,D.A., Valentine,B.A., Combs,G.F. and Lei,X.G. (1997) Cellular glutathione peroxidase knockout mice express normal levels of selenium-dependent plasma and phospholipid hydroperoxide glutathione peroxidases in various tissues. *J. Nutr.*, **127**, 1445–1450.
21. Fomenko,D.E., Novoselov,S.V., Natarajan,S.K., Lee,B.C., Koc,A., Carlson,B.A., Lee,T.H., Kim,H.Y., Hatfield,D.L. and Gladyshev,V.N. (2009) MsrB1 (methionine-R-sulfoxide reductase 1) knock-out mice: roles of MsrB1 in redox regulation and identification of a novel selenoprotein form. *J. Biol. Chem.*, **284**, 5986–5993.
22. Ho,Y.S., Magnenat,J.L., Bronson,R.T., Cao,J., Gargano,M., Sugawara,M. and Funk,C.D. (1997) Mice deficient in cellular glutathione peroxidase develop normally and show no increased sensitivity to hyperoxia. *J. Biol. Chem.*, **272**, 16644–16651.
23. Lei,X.G., Evenson,J.K., Thompson,K.M. and Sunde,R.A. (1995) Glutathione peroxidase and phospholipid hydroperoxide glutathione peroxidase are differentially regulated in rats by dietary selenium. *J. Nutr.*, **125**, 1438–1446.
24. Hadley,K.B. and Sunde,R.A. (2001) Selenium regulation of thioredoxin reductase activity and mRNA levels in rat liver. *J. Nutr. Biochem.*, **12**, 693–702.
25. Jeong,D.W., Kim,E.H., Kim,T.S., Chung,Y.W., Kim,H. and Kim,I.Y. (2004) Different distributions of selenoprotein W and thioredoxin during postnatal brain development and embryogenesis. *Mol. Cells*, **17**, 156–159.
26. Jakupoglu,C., Przemeck,G.K., Schneider,M., Moreno,S.G., Mayr,N., Hatzopoulos,A.K., de Angelis,M.H., Wurst,W., Bornkamm,G.W., Brielmeier,M. *et al.* (2005) Cytoplasmic thioredoxin reductase is essential for embryogenesis but dispensable for cardiac development. *Mol. Cell. Biol.*, **25**, 1980–1988.
27. Yant,L.J., Ran,Q., Rao,L., Van Remmen,H., Shibatani,T., Belter,J.G., Motta,L., Richardson,A. and Prolla,T.A. (2003) The selenoprotein GPX4 is essential for mouse development and protects from radiation and oxidative damage insults. *Free Radic. Biol. Med.*, **34**, 496–502.
28. Walczak,R., Westhof,E., Carbon,P. and Krol,A. (1996) A novel RNA structural motif in the selenocysteine insertion element of eukaryotic selenoprotein mRNAs. *RNA*, **2**, 367–379.
29. Fagegaltier,D., Lescure,A., Walczak,R., Carbon,P. and Krol,A. (2000) Structural analysis of new local features in SECIS RNA hairpins. *Nucleic Acids Res.*, **28**, 2679–2689.
30. Grundner-Culemann,E., Martin,G.W. 3rd, Harney,J.W. and Berry,M.J. (1999) Two distinct SECIS structures capable of directing selenocysteine incorporation in eukaryotes. *RNA*, **5**, 625–635.
31. Miniard,A.C., Middleton,L.M., Budiman,M.E., Gerber,C.A. and Driscoll,D.M. (2010) Nucleolin binds to a subset of selenoprotein mRNAs and regulates their expression. *Nucleic Acids Res.*, **38**, 4807–4820.
32. Fletcher,J.E., Copeland,P.R., Driscoll,D.M. and Krol,A. (2001) The selenocysteine incorporation machinery: interactions between the SECIS RNA and the SECIS-binding protein SBP2. *RNA*, **7**, 1442–1453.
33. Mehta,A., Rebsch,C.M., Kinzy,S.A., Fletcher,J.E. and Copeland,P.R. (2004) Efficiency of mammalian selenocysteine incorporation. *J. Biol. Chem.*, **279**, 37852–37859.
34. Walczak,R., Carbon,P. and Krol,A. (1998) An essential non-Watson-Crick base pair motif in 3′UTR to mediate selenoprotein translation. *RNA*, **4**, 74–84.
35. Martin,G.W. 3rd, Harney,J.W. and Berry,M.J. (1998) Functionality of mutations at conserved nucleotides in eukaryotic SECIS elements is determined by the identity of a single nonconserved nucleotide. *RNA*, **4**, 65–73.
36. Schneider,M.J., Fiering,S.N., Thai,B., Wu,S.Y., St Germain,E., Parlow,A.F., St Germain,D.L. and Galton,V.A. (2006) Targeted disruption of the type 1 selenodeiodinase gene (Dio1) results in marked changes in thyroid hormone economy in mice. *Endocrinology*, **147**, 580–589.
37. Allamand,V., Richard,P., Lescure,A., Ledeuil,C., Desjardin,D., Petit,N., Gartioux,C., Ferreiro,A., Krol,A., Pellegrini,N. *et al.* (2006) A single homozygous point mutation in a 3′untranslated region motif of selenoprotein N mRNA causes SEPN1-related myopathy. *EMBO Rep.*, **7**, 450–454.
38. Moghadaszadeh,B., Petit,N., Jaillard,C., Brockington,M., Roy,S.Q., Merlini,L., Romero,N., Estournet,B., Desguerre,I., Chaigne,D. *et al.* (2001) Mutations in SEPN1 cause congenital muscular dystrophy with spinal rigidity and restrictive respiratory syndrome. *Nat. Genet.*, **29**, 17–18.
39. Dikiy,A., Novoselov,S.V., Fomenko,D.E., Sengupta,A., Carlson,B.A., Cerny,R.L., Ginalski,K., Grishin,N.V.,

Hatfield,D.L. and Gladyshev,V.N. (2007) SelT, SelW, SelH, and Rdx12: genomics and molecular insights into the functions of selenoproteins of a novel thioredoxin-like family. *Biochemistry*, **46**, 6871–6882.
40. Barnes,K.M., Evenson,J.K., Raines,A.M. and Sunde,R.A. (2009) Transcript analysis of the selenoproteome indicates that dietary selenium requirements of rats based on selenium-regulated selenoprotein mRNA levels are uniformly less than those based on glutathione peroxidase activity. *J. Nutr.*, **139**, 199–206.
41. Kryukov,G.V., Castellano,S., Novoselov,S.V., Lobanov,A.V., Zehtab,O., Guigo,R. and Gladyshev,V.N. (2003) Characterization of mammalian selenoproteomes. *Science*, **300**, 1439–1443.
42. Oguro,A., Ohtsu,T., Svitkin,Y.V., Sonenberg,N. and Nakamura,Y. (2003) RNA aptamers to initiation factor 4A helicase hinder cap-dependent translation by blocking ATP hydrolysis. *RNA*, **9**, 394–407.
43. Del Campo,M. and Lambowitz,A.M. (2009) Structure of the Yeast DEAD box protein Mss116p reveals two wedges that crimp RNA. *Mol. Cell*, **35**, 598–609.
44. Sengoku,T., Nureki,O., Nakamura,A., Kobayashi,S. and Yokoyama,S. (2006) Structural basis for RNA unwinding by the DEAD-box protein Drosophila Vasa. *Cell*, **125**, 287–300.
45. Sauliere,J., Haque,N., Harms,S., Barbosa,I., Blanchette,M. and Le Hir,H. (2010) The exon junction complex differentially marks spliced junctions. *Nat. Struct. Mol. Biol.*, **17**, 1269–1271.